

1 **Supplementary Material for**

2 **Long-term Sorption of Lincomycin to Biochars: The Intertwined Roles of Pore Diffusion**

3 **and Dissolved Organic Carbon**

4 Cheng-Hua Liu^{a, b}, Ya-Hui Chuang^{a, c}, Hui Li^a, Stephen A. Boyd^a, Brian J. Teppen^a, Javier

5 M. Gonzalez^d, Cliff T. Johnston^e, Johannes Lehmann^f, and Wei Zhang^{a, b, *}

6 ^a Department of Plant, Soil and Microbial Sciences, Michigan State University, East Lansing,

7 Michigan 48824, United States

8 ^b Environmental Science and Policy Program, Michigan State University, East Lansing,

9 Michigan 48824, United States

10 ^c Department of Soil and Environmental Sciences, National Chung-Hsing University, Taichung

11 402, Taiwan

12 ^d National Soil Erosion Research Lab, Agricultural Research Service, United States Department

13 of Agriculture, West Lafayette, IN 47907, United States

14 ^e Department of Agronomy, Purdue University, West Lafayette, IN 47907, United States

15 ^f Soil and Crop Sciences Section, School of Integrative Plant Science, Cornell University, Ithaca,

16 NY 14853, United States

17 *Corresponding author: Dr. Wei Zhang, Address: 1066 Bogue ST RM A516, East Lansing, MI

18 48824, United States; Tel: 517-353-0471; Fax: 517-355-0270; Email: weizhang@msu.edu

19 Submitted to *Water Research*

20 **Content**

21 S1. Supplemental Materials and Methods

22 S2. Supplemental Results and Discussions

23 28 pages, 13 figures, and 6 tables

24 **S1. Supplemental Materials and Methods**

25 **Sorbent characterization.** Surface area and porosity of biochars were determined by
26 CO₂ adsorption isotherms at 273 K in the relative pressure (P/P_0) range of 0.004 to 0.032.
27 Specific surface area (SSA) and micropore volume (V_{mic}) were then calculated based on the
28 Langmuir equation and the Dubinin-Astakhov equation, respectively. Prior to CO₂ adsorption, all
29 biochars were degassed at 300 °C for 12 hours under N₂ so that the vapor emission from biochars
30 was sufficiently low to perform the measurement. It was noted that the used degassing
31 temperature and duration could potentially increase the surface area and pore volume of biochars
32 due to the removal of poorly-carbonized fraction during degassing (Sigmund et al., 2017)
33 because biochar surface and pores originally clogged by volatiles become more accessible. As a
34 result, the actual surface area and porosity of biochars may be overestimated. Measuring the
35 change of surface area and porosity of biochars due to the release of dissolved organic carbon
36 (DOC) is important to studying the underlying sorption mechanisms. To limit the loss of DOC
37 during degassing, relatively lower degassing temperature and longer degassing duration were
38 used in our preliminary test. However, the preliminary determination of surface area and porosity
39 by N₂ adsorption at 77 K for BM300 (a poorly-carbonized biochar sample) was not successful
40 following degassing at 150 °C for 48 hours under vacuum, which was attributed to the
41 interference from a continuous emission of volatile organic compounds from the leachable DOC
42 and poorly-carbonized organic fractions in biochars during measurement. Since we were not able
43 to successfully measure surface area and porosity of biochars without removing volatiles by
44 degassing, the determination of detailed pore size distribution before and after the DOC release
45 was not performed in this study.

46 **Biochar Suspensions.** To generate a biochar suspension for the zeta potential
47 measurements, 8 mg each biochar was mixed with 8 mL 0.02 M background electrolyte (6.7 mM
48 NaCl, 2.5 mM Na₂CO₃, 2.5 mM NaHCO₃, and 200 mg L⁻¹ NaN₃.) in amber glass vials and then
49 shaken end-over-end for 1 day. Afterwards, the vials were allowed standing for 30 min and then
50 the top 1 mL of the suspension was withdrawn and measured for the zeta potential by the
51 Zetasizer Nano-ZS. The remained suspensions were used to determine solution pH of the
52 suspension (10.0 ± 0.1 for all tested biochars).

53 To measure the biochar colloid size after the DOC release, biochars were suspended in
54 0.01M NaCl or 0.01M NaOH solution (1:1 solid/water ratio) and shaken end-over-end for 1 day.
55 After shaking, the vials were allowed standing for 30 min and then the top 1 mL of the biochar
56 suspension was withdrawn and measured for particle size by the Zetasizer Nano-ZS.

57 **Determination of Lincomycin Concentrations.** The concentration of lincomycin in
58 solutions were determined by a Shimadzu Prominence high-performance liquid chromatograph
59 coupled to an Applied Biosystems Sciex 3200 triple quadrupole mass spectrometer (LC-MS/MS)
60 (Chuang et al., 2015). The analytical column was an Agilent ZORBAX Eclipse Plus C18 column
61 (Agilent Technologies, Santa Clara, CA, USA) with 50 mm length × 2.1 mm diameter and 5 μm
62 particle size. The mobile phase A consisted of DI water and 0.3% formic acid. The mobile phase
63 B consisted of 1:1 (v/v) acetonitrile-methanol mixture and 0.3% formic acid. Data were acquired
64 using a gradient condition of 0–40% B in 0–1 min, 40–70% B in 1–2 min, 70–80% B in 2–3 min,
65 80–100% B in 3–3.5 min, and 100% B for 0.5 min. The flow rate was set to 0.35 mL min⁻¹ and
66 the injection volume was set to 10 μL. The electrospray ionization (ESI) in positive ion mode was
67 used in the tandem quadrupole MS. Lincomycin was detected and quantified using a multiple

68 reaction monitoring mode with a precursor/product transition of 407.2/126.2. The retention time
69 was 2.37 min and the instrument detection limit of lincomycin was 0.2 pg.

70 **Determination of DOC Concentration.** The concentration of DOC released from the
71 biochars were determined by our recently developed UV absorption method with a Varian Cary
72 50 Bio UV-visible spectrophotometer (Liu et al., 2019). We considered the biochar DOC was a
73 mixture of the acid-soluble (AS) and acid-precipitable (AP) fractions and the fraction of AS can
74 be calculated via:

$$75 \quad f_{AS} = \frac{1.135e^{-2.813}}{e^{-1.797}} \quad (1)$$

76 where f_{AS} is the proportion of the AS fraction ($0 \leq f_{AS} \leq 1$), and e is the E_2/E_3 ratio. The E_2/E_3
77 ratio was calculated as the ratio of decadic absorption coefficient (a , cm^{-1}) at 254 nm (a_{254}) to
78 365 nm (a_{365}), where the a was calculated by UV-vis absorbance (unitless) divided by path
79 length (cm). If calculated f_{AS} value is < 0 or > 1 , it will be assumed to be 0 or 1, respectively.
80 Then, the biochar DOC concentration in solution (in the unit of mg-C L^{-1}) can be calculated via:

$$81 \quad \text{DOC} = \frac{\alpha_{254}}{0.0232f_{AS} + 0.0642(1-f_{AS})} \quad (2)$$

82 The DOC determined by the UV absorption method was generally in good agreement with
83 the DOC measured by a total organic carbon (TOC) analyzer. The instrument detection limit of
84 UV-visible spectrophotometer was 0.0037 cm^{-1} at 254 nm and 0.0030 cm^{-1} at 365 nm.

85 **Effect of Biochar-DOC as Co-solute on Lincomycin Sorption.** To extract the DOC
86 from the biochars, 500 mg of each selected biochar were mixed with 50 mL of DI water in 50
87 mL polypropylene (PP) centrifuge tubes, and then shaken end-over-end at 30 rpm in dark for 7
88 days. Afterwards the tubes were centrifuged at $8,000 \times g$ for 20 min, and the supernatants were
89 then vacuum-filtered through a $0.45\text{-}\mu\text{m}$ membrane (mixed cellulose esters). The final filtrates
90 were collected as the DOC stock solutions, and the DOC concentrations were determined by a

91 Shimadzu TOC-V_{CPN} TOC analyzer (Shimadzu, Japan). Aliquots of each DOC stock solutions
92 were further diluted 10-fold with a lincomycin solution (lincomycin concentration of 1111 μg
93 L^{-1} and ionic strength of 0.022 M background electrolytes) to achieve the initial lincomycin
94 concentration of 1000 μg L^{-1} , ionic strength of 0.02 M, and DOC concentration of 17.2, 7.94,
95 11.1, and 10.9 mg-C L^{-1} for BM300-, DM300-, PM300-, and DDM500-DOC, respectively. For
96 comparison, a lincomycin solution without DOC was prepared using the same protocol but
97 replacing the DOC stock solution with DI water. The prepared lincomycin solutions with and
98 without DOC were denoted as lincomycin/DOC and lincomycin/DI, respectively. Thereafter, the
99 lincomycin sorption kinetics in the presence of DOC were carried out using WW500 biochar,
100 which was selected because of its low DOC content. Briefly, 8 mL of each lincomycin/DOC and
101 lincomycin/DI solutions were mixed with 8 mg WW500 biochar in vials, and then the vials were
102 shaken end-over-end at 30 rpm in dark for the duration of 1 day to 60 days. The other procedures
103 were same as described in the sorption kinetics section. In addition, the control experiments of
104 lincomycin/DOC solutions without WW500 biochars were also performed using the same
105 protocol.

106 **Lincomycin Sorption to Washed Biochars.** To wash out the DOC, 500 mg of each
107 selected biochar (BM300, BM600, DM300, PM300, and DDM500) were mixed with 50 mL of
108 0.1 M NaOH (only for BM300, BM600, and DM300) or DI water in vials and then end-over-end
109 shaken at 30 rpm in dark for 1 day or 40 days, respectively. The suspensions were then
110 centrifuged at $8,000 \times g$ for 20 min, and the supernatant was collected. The supernatant was
111 vacuum-filtered through a 0.45- μm membrane and determined for the DOC concentration by the
112 TOC analyzer after appropriate sample dilution. The treated biochar pellets were re-dispersed
113 with 50 mL DI water and re-centrifuged for five times to remove remaining salt and DOC, and

114 then freeze-dried to obtain the DOC-washed biochars. The sorption kinetics of lincomycin on the
115 washed biochars were conducted as previously describe. Briefly, 8 mg of each washed biochar
116 were suspended in 8 mL of $1000 \mu\text{g L}^{-1}$ lincomycin solution, and then end-over-end shaken at 30
117 rpm in dark for the duration of 1 to 30 days. The rest sampling and analysis procedures were
118 identical as previously described.

119 **Lincomycin Binding to Biochar-DOC in Solution.** Briefly, 7.2 mL of each DI-water-
120 extracted DOC solution as described above (40-d extraction) was mixed with 0.8 mL of
121 lincomycin solution (lincomycin concentration of $10,000 \mu\text{g L}^{-1}$ and ionic strength of 0.2 M
122 background electrolytes) in vials to acquire the lincomycin/DOC mixture solution with the initial
123 lincomycin concentration of $1000 \mu\text{g L}^{-1}$, ionic strength of 0.02 M, and DOC concentration of
124 186, 93.8, 97.4, and 89.6 mg-C L^{-1} for BM300-, DM300-, PM300-, and DDM500-DOC,
125 respectively. The vials were then end-over-end shaken at 30 rpm in dark for 1 day. Afterwards,
126 the lincomycin/DOC mixture solution was passed through an Oasis hydrophilic–lipophilic
127 balance (HLB) cartridge (Waters, Milford, MA, USA), which was preconditioned with 3.0 mL of
128 methanol and 3.0 mL of DI water. At this step, the DOC-bound lincomycin in solution could
129 pass through the HLB cartridge and the freely dissolved lincomycin in solution would be
130 retained by the HLB cartridge. The retained freely-dissolved lincomycin was further eluted from
131 the HLB cartridge with 5.0 mL of methanol, and then determined the concentration by LC-
132 MS/MS. Finally, the DOC-bound lincomycin concentration was calculated by the difference
133 between initial applied lincomycin concentration and freely dissolved lincomycin concentration
134 in solutions.

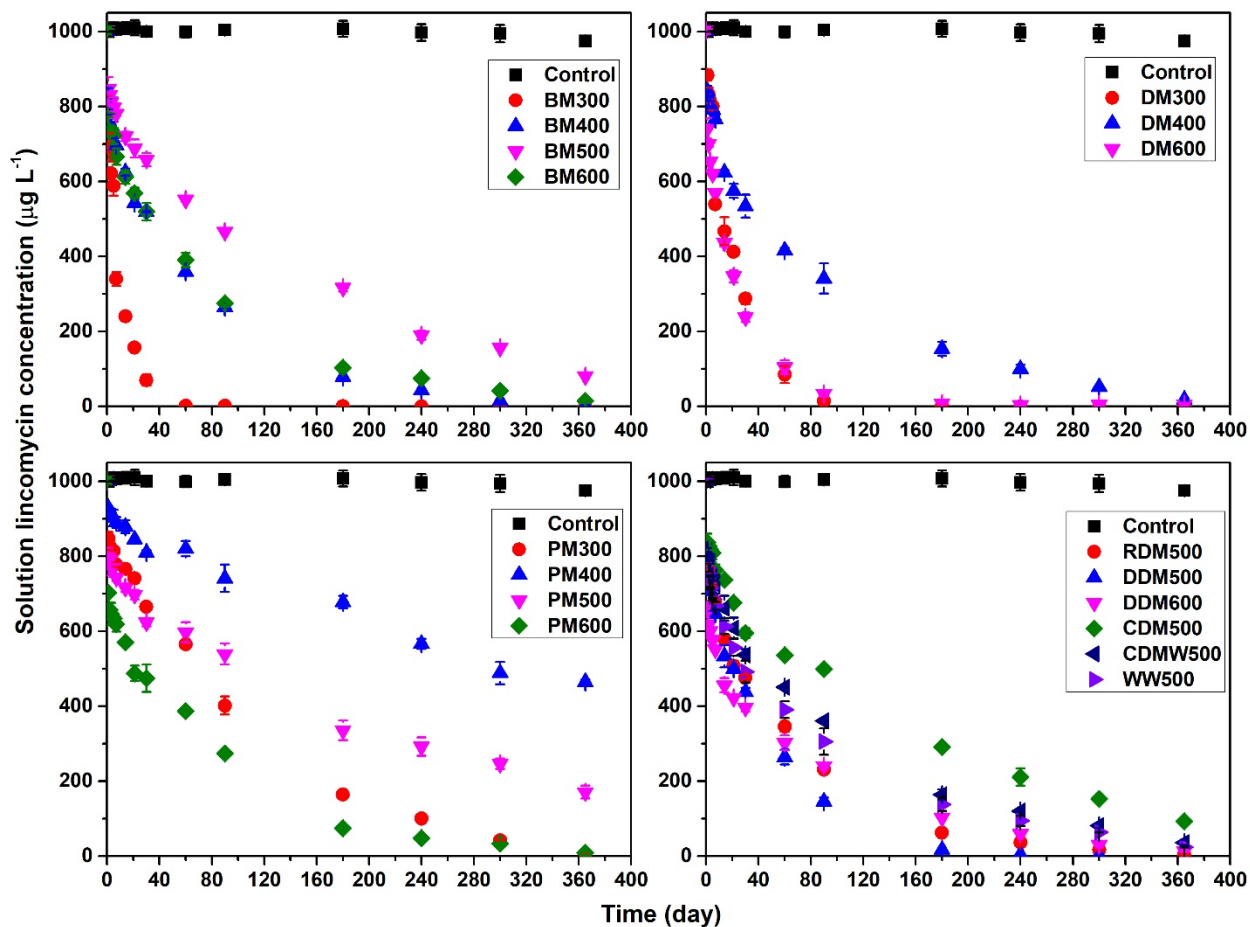
135 **Extraction of Sorbed Lincomycin.** Following the sorption kinetics after 240 days (when
136 over 70% of tested biochars were approaching the apparent sorption equilibrium), two vials of

137 each biochar in the kinetic sorption experimental set were retrieved. The suspensions in vials
138 were stirred with a PTFE-coated micro stir bar, and 2 mL of each suspension was uniformly
139 withdrawn, filtered, and determined for the lincomycin concentration in filtrates by the LC-
140 MS/MS. In addition, another 1 mL of each suspension was placed into a vial containing 4 mL of
141 acetonitrile/methanol (8/2 in v/v) extraction solvent. The vials were end-over-end shaken at 30
142 rpm in dark for 7 days and then sonicated in ultrasonic bath (Model FS110H, Fisher Scientific,
143 Pittsburgh, PA, USA) for 60 min at 50 °C. The suspensions were then centrifuged, filtered, and
144 determined for the lincomycin concentration by the LC-MS/MS as described previously. The
145 extraction recovery of lincomycin from biochars were calculated by mass balance.

146 To examine the effect of sorption equilibration time on the extraction recovery of sorbed
147 lincomycin on the biochars, 8 mg of DM600 biochar sample were added into 8 mL of
148 lincomycin solution with an initial concentration of 500 $\mu\text{g L}^{-1}$, initial pH of 10, and ionic
149 strength of 0.02 M. The suspensions were end-over-end shaken at 30 rpm in dark for 1, 4, and 30
150 days. The other sorption/extraction procedures were identical as described earlier, except for a
151 shorter extraction time of 1 day.

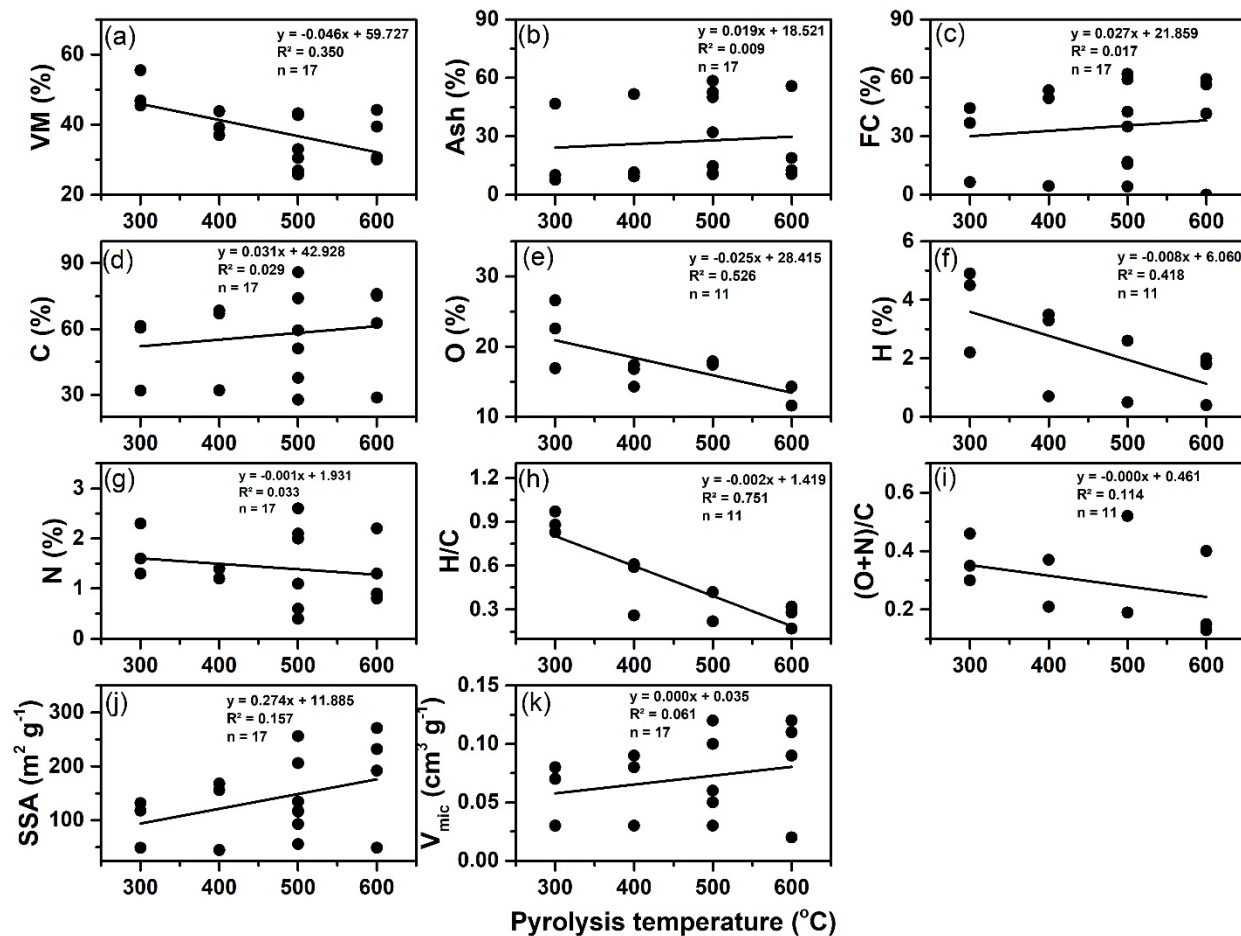
152

153 S2. Supplemental Results and Discussion



154
155 **Figure S1.** Lincomycin concentrations in solution over time in the kinetic sorption experiments
156 for the 17 tested biochars. Control was the biochar-free lincomycin solution.

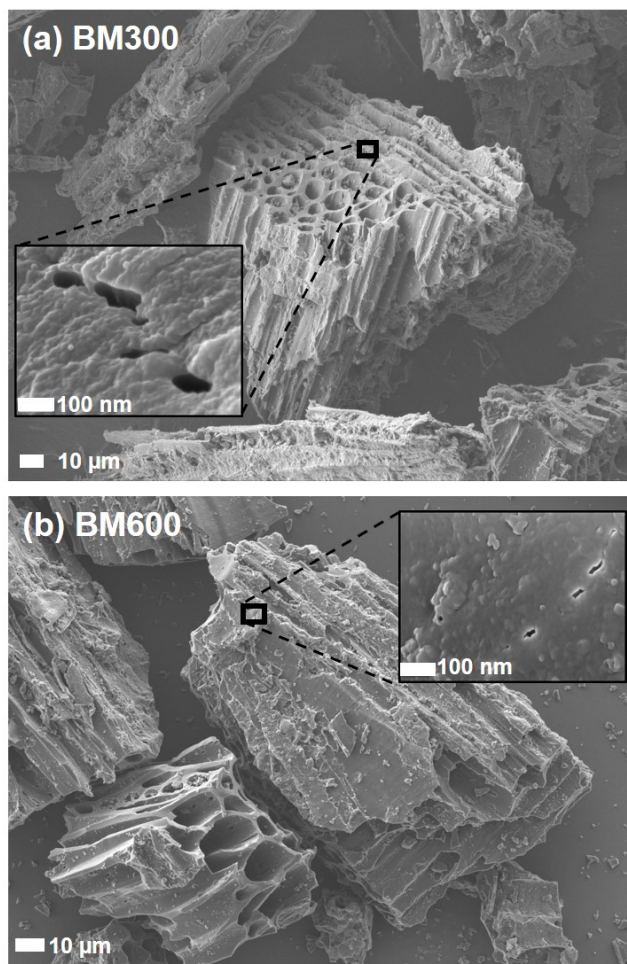
157



158

159 **Figure S2.** Relationship of (a) volatile matter (VM) content, (b) Ash content, (c) fixed carbon
 160 (FC) content, (d) total C content, (e) total O content, (f) total H content, (g) total N content, (h)
 161 H/C atomic ratio, (i) (O+N)/C atomic ratio, (j) specific surface area (SSA), and (k) micropore
 162 volume (V_{mic}) versus pyrolysis temperature of biochars.

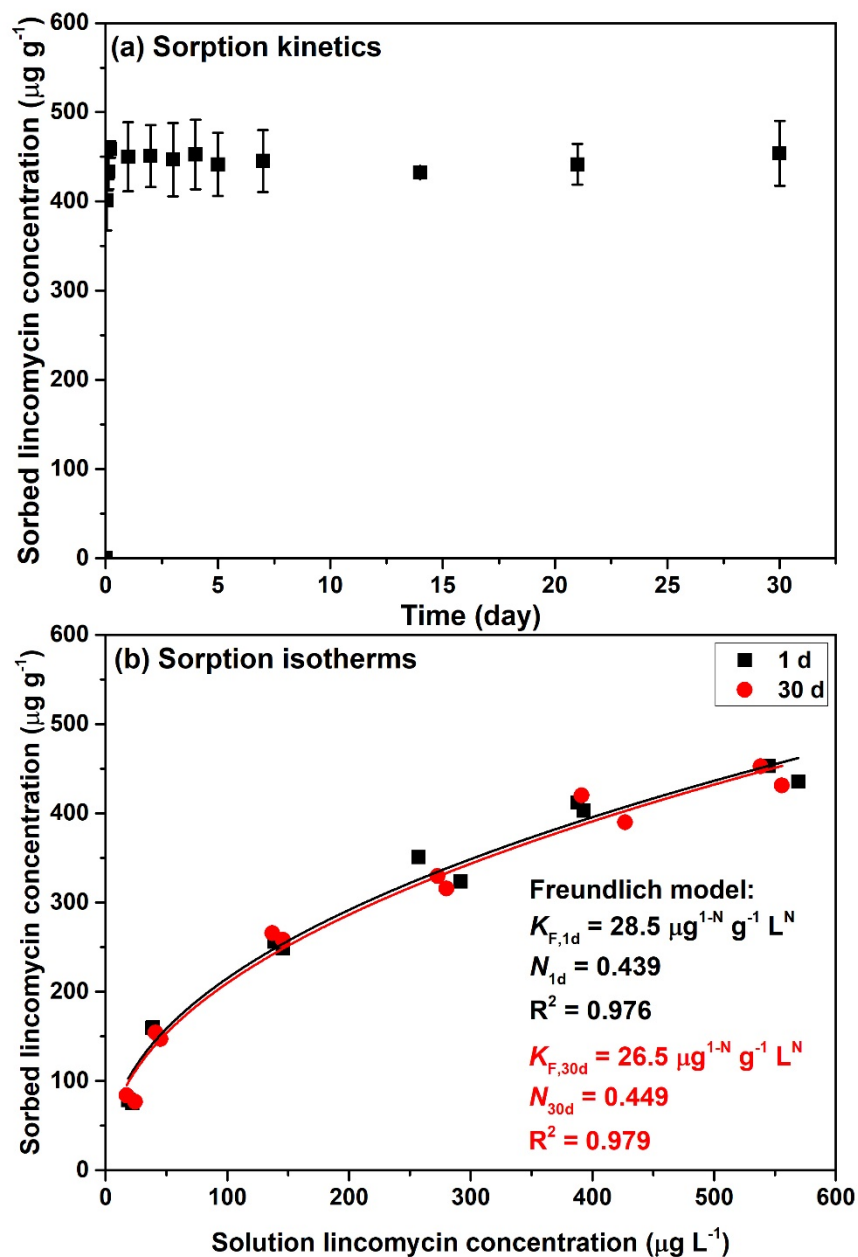
163



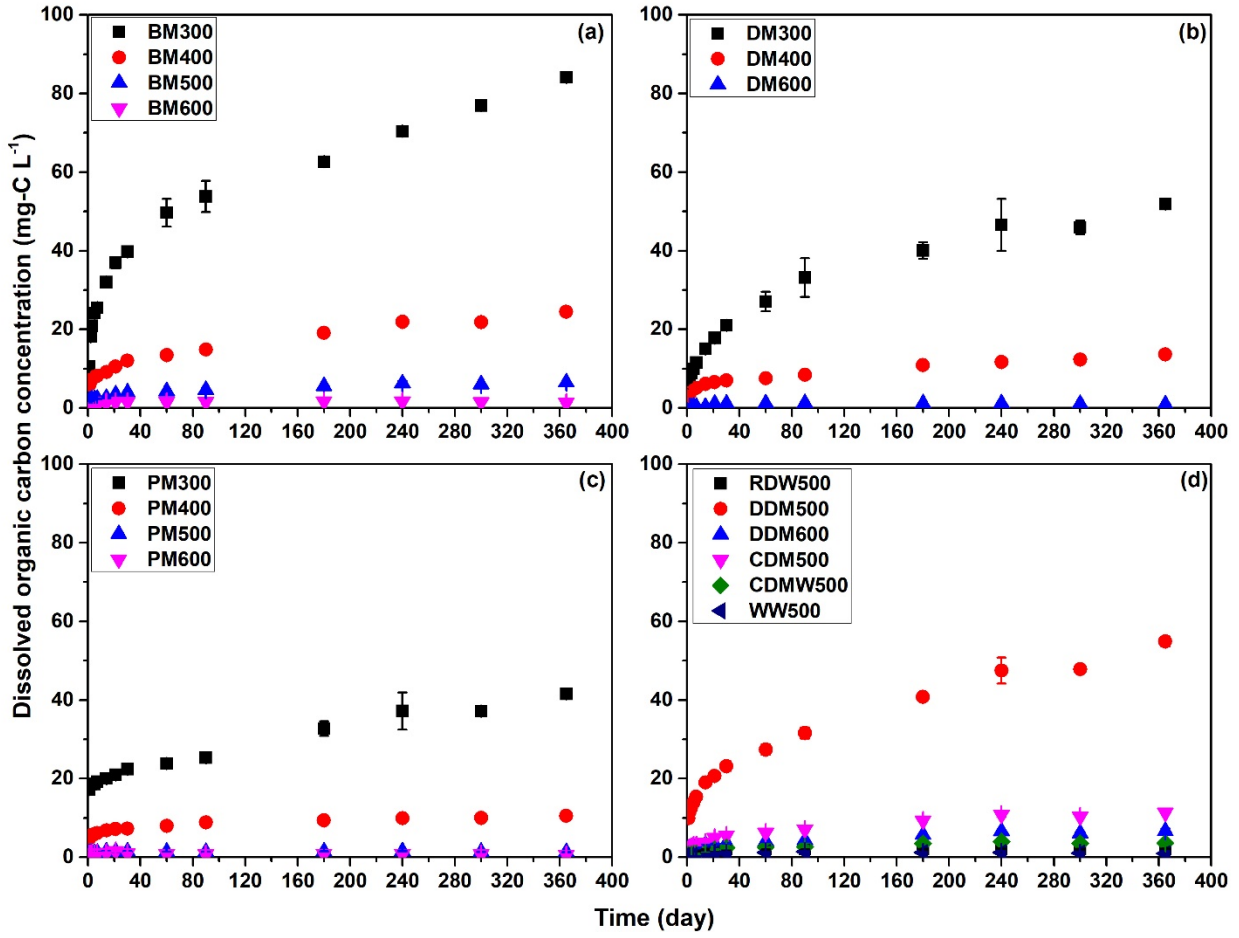
164

165 **Figure S3.** Scanning electron microscopy images of raw biochars: (a) BM300 (bull manure
166 biochar produced at 300 °C) and (b) BM600 (bull manure biochar produced at 600 °C).

167

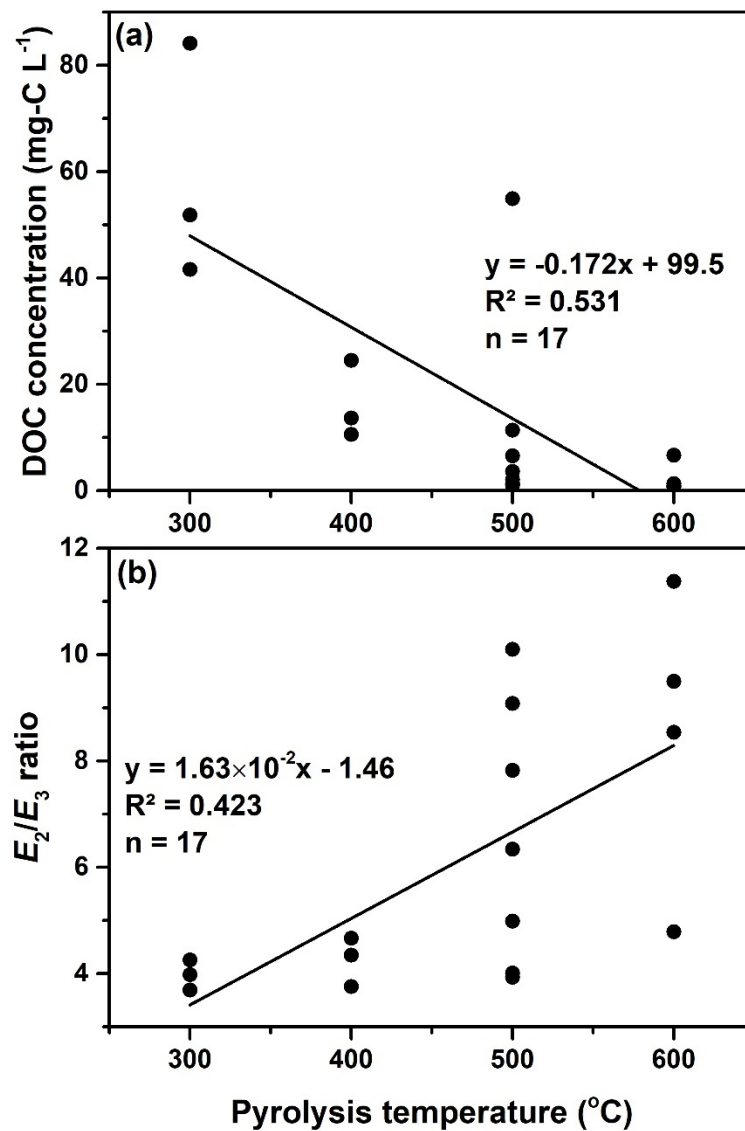


168
 169 **Figure S4.** Sorption kinetics (a) and isotherms (b) of lincomycin to graphite. The solid lines
 170 were fitted by the Freundlich model. The K_d values were 28.5 L g^{-1} (1-d sorption equilibration
 171 time) and 26.5 L g^{-1} (30-d sorption equilibration time) at $C_w = 1 \mu\text{g L}^{-1}$.



172

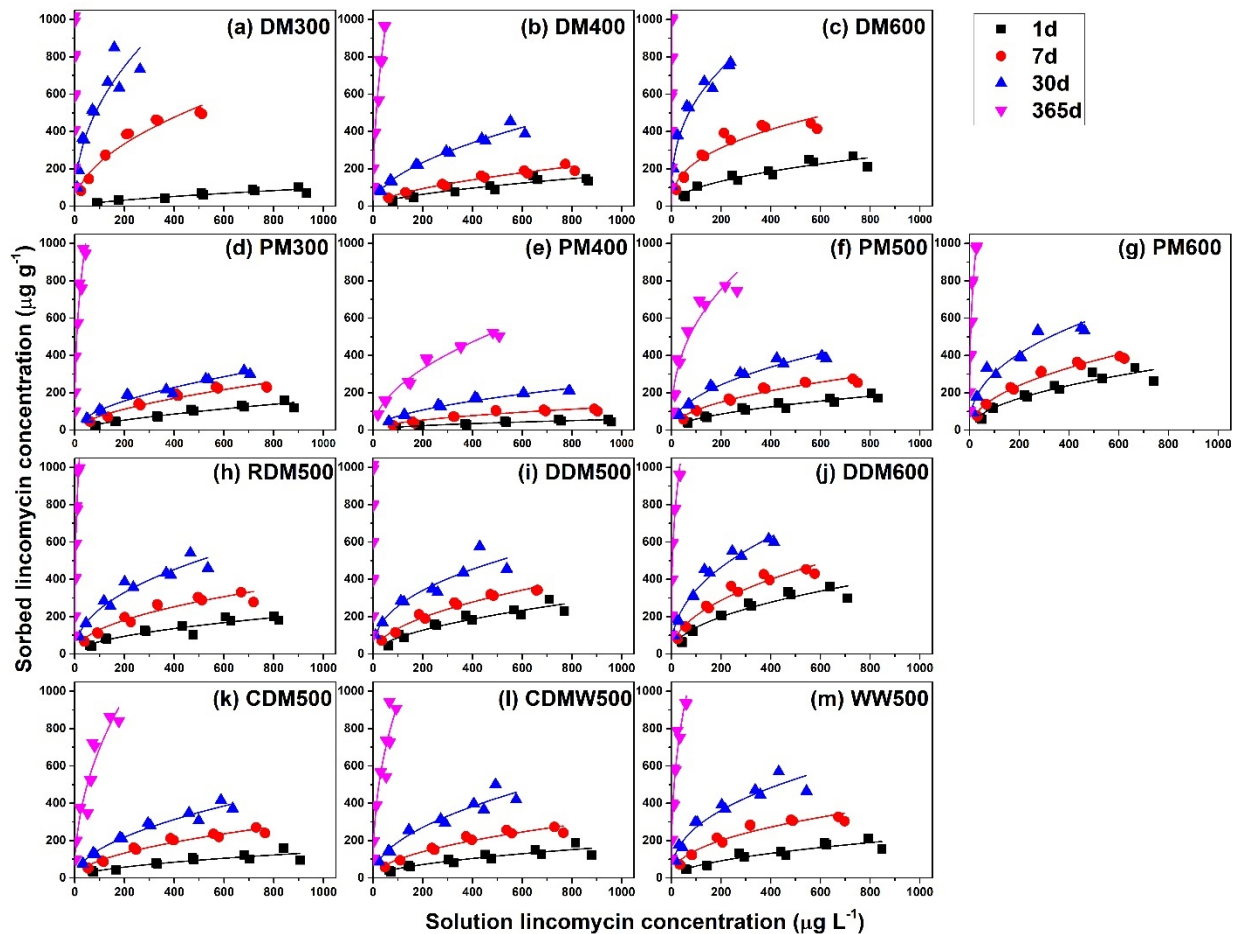
173 **Figure S5.** Long-term release of dissolved organic carbon from biochars.



174

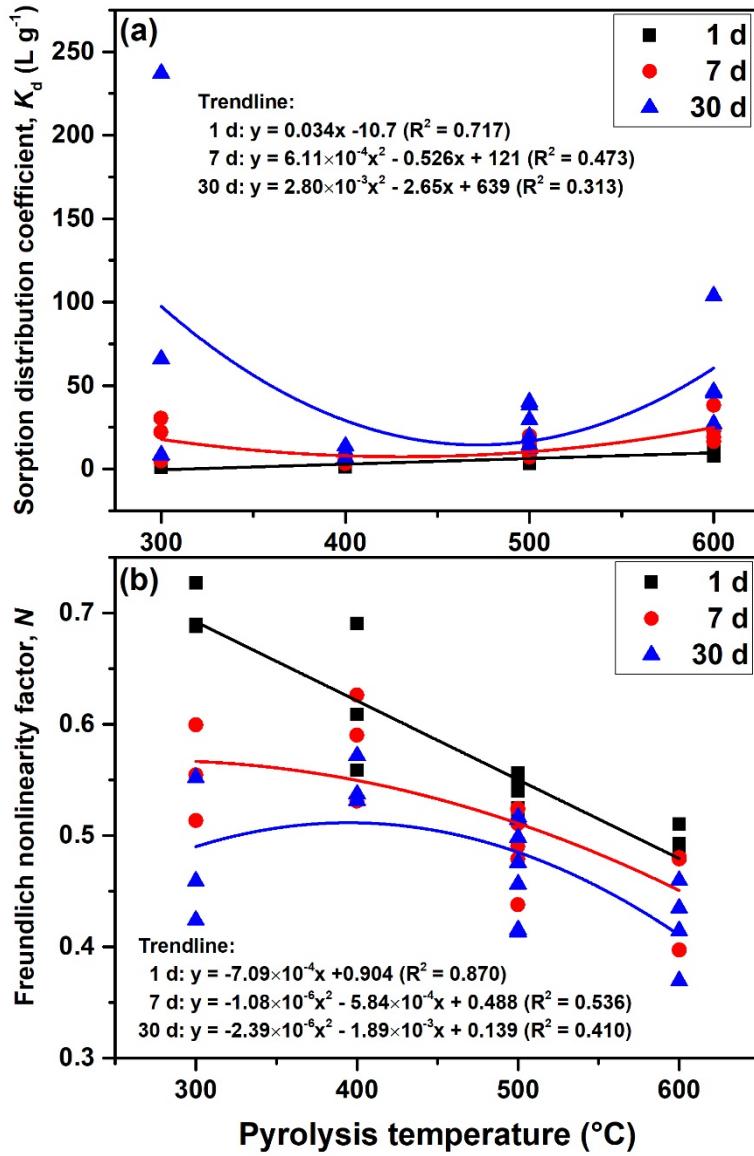
175 **Figure S6.** The relationship of concentration (a) and E_2/E_3 ratio (b) of biochar-DOC versus
 176 pyrolysis temperature. The tested biochar-DOC samples were collected from long-term sorption
 177 kinetics at 365 days.

178



179
 180 **Figure S7.** Quasi-equilibrium sorption isotherms of lincomycin to biochars at 1, 7, 30, and 365
 181 days: (a) DM300, (b) DM400, (c) DM600, (d) PM300, (e) PM400, (f) PM500, (g) PM600, (h)
 182 RDM500, (i) DDM500, (j) DDM600, (k) CDM500, (l) CDMW500, and (m) WW500. The solid
 183 lines were fitted with the Freundlich isotherm model.

184

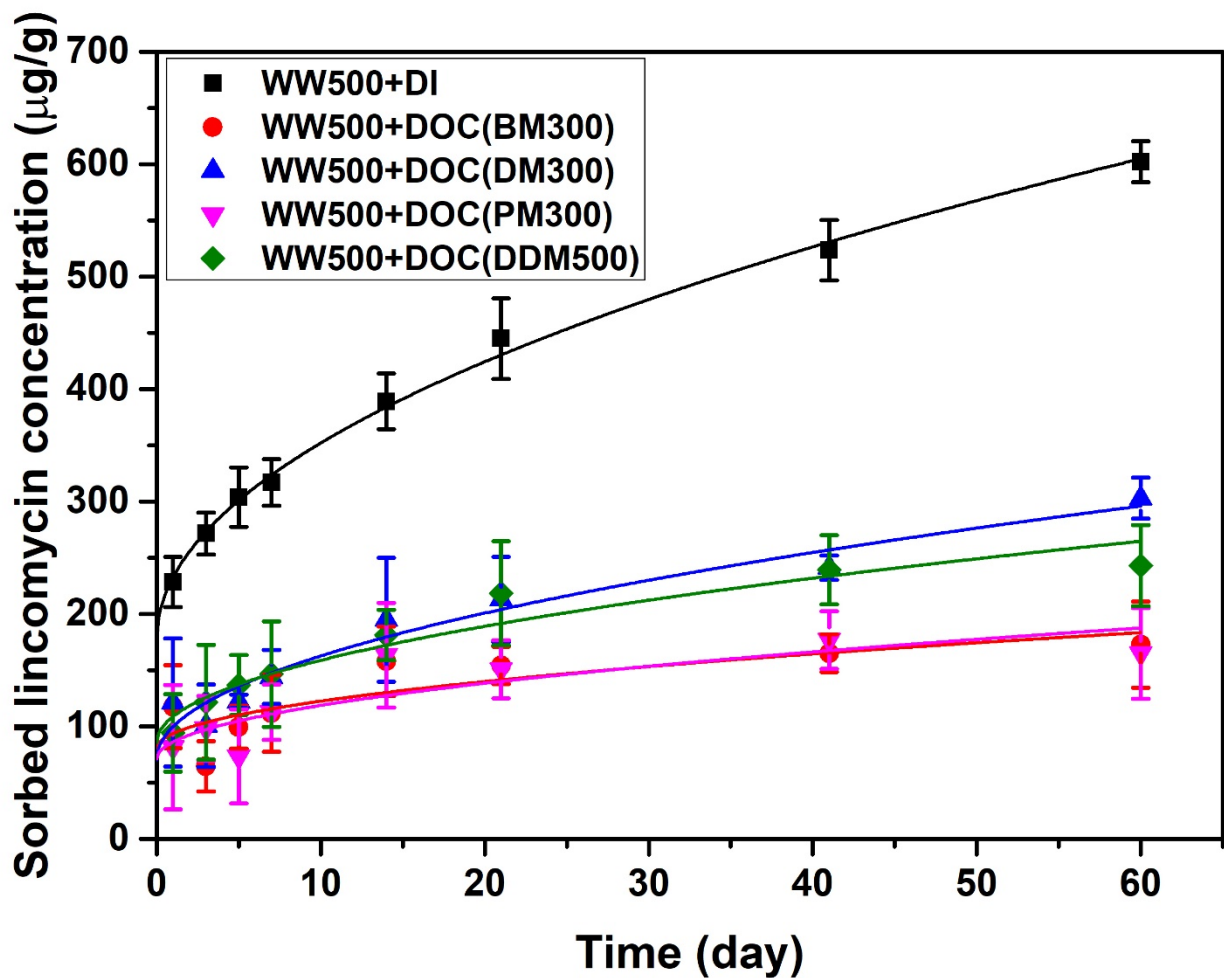


185

186 **Figure S8.** The relationship of sorption distribution coefficient (K_d) and Freundlich nonlinearity

187 factor (N) versus pyrolysis temperature for biochars.

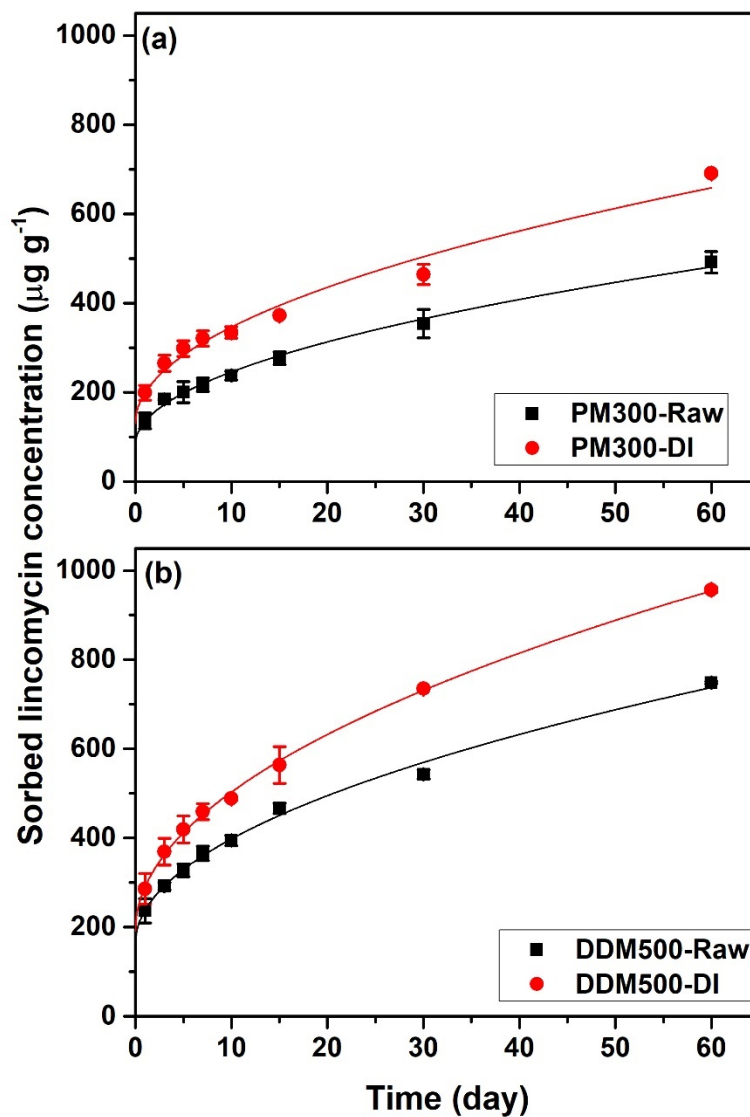
188



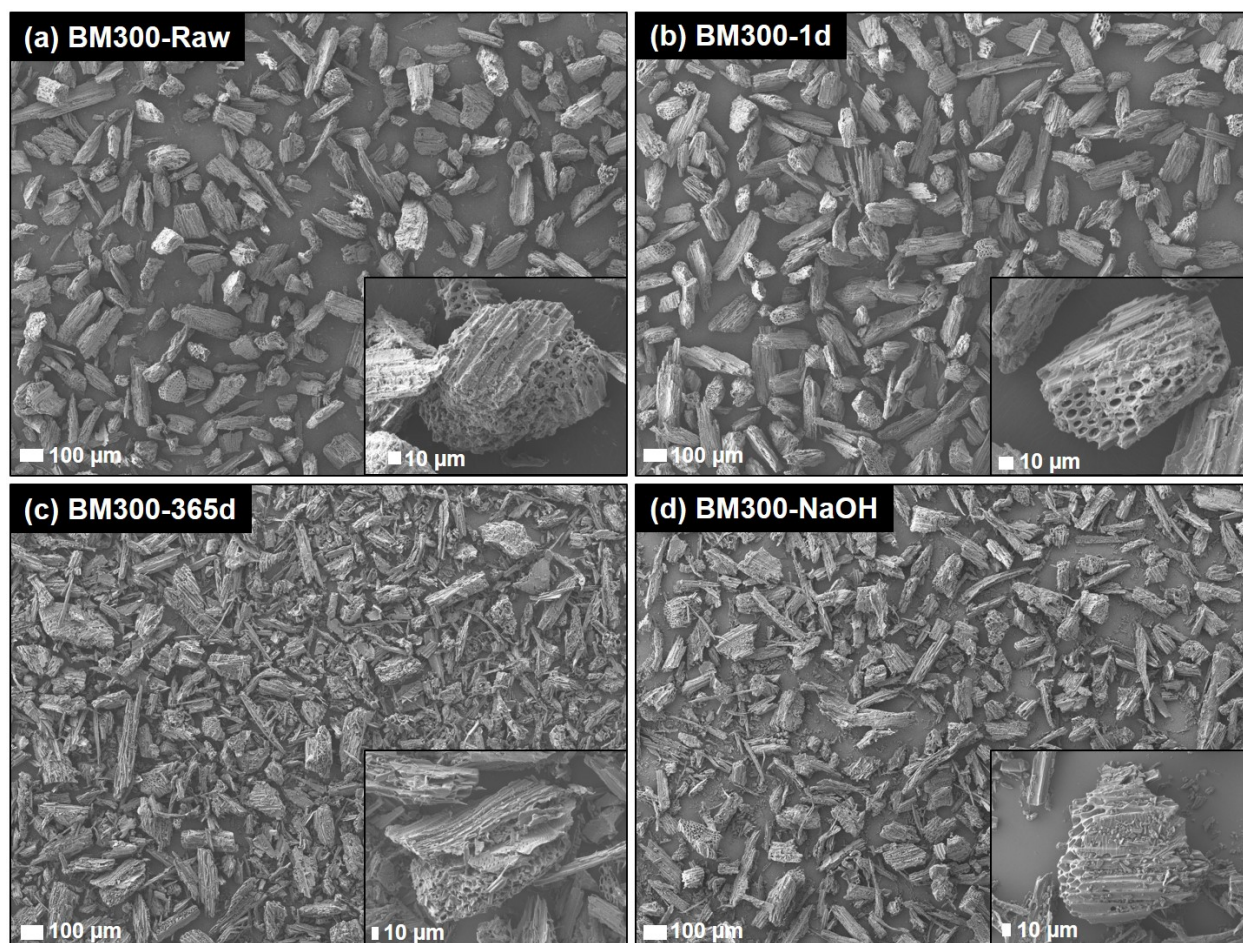
189

190 **Figure S9.** The effect of biochar-derived DOC as co-solutes on sorption kinetics of lincomycin
 191 by WW500 biochar (WW500+DI was the control of absence DOC). The sorption data were
 192 fitted by the intraparticle diffusion model (solid line). The symbols and error bars represent mean
 193 and standard deviation of duplicates.

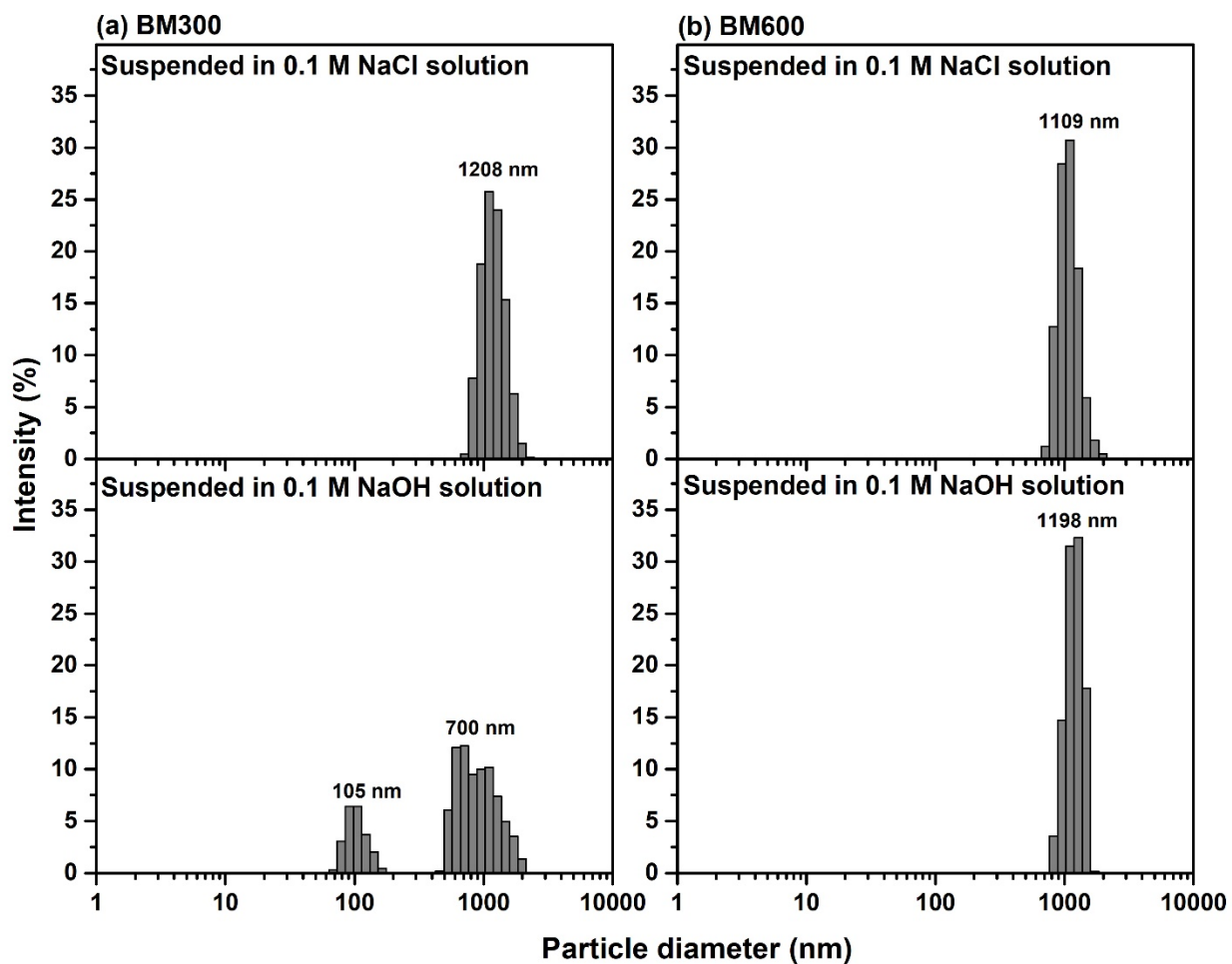
194



195
 196 **Figure S10.** Long-term kinetics of lincomycin sorption by raw- and DI-water-washed biochars:
 197 (a) PM300 and (b) DDM500. The sorption data were fitted by the intraparticle diffusion model
 198 (solid line). The symbols and error bars represent mean and standard deviation of duplicates.



199
200 **Figure S11.** Scanning electron microscopy images of bull manure biochar pyrolyzed at 300°C
201 (BM300): (a) raw BM300 without treatment, (b) BM300 after 1-d background solution exposure,
202 (c) BM300 after 365-d background solution exposure, and (d) BM300 after 1-d 0.1 M NaOH
203 solution exposure. Background solution contained 1000 $\mu\text{g L}^{-1}$ lincomycin, 6.7 mM NaCl, 2.5
204 mM Na_2CO_3 , 2.5 mM NaHCO_3 , and 200 mg L^{-1} NaN_3 .

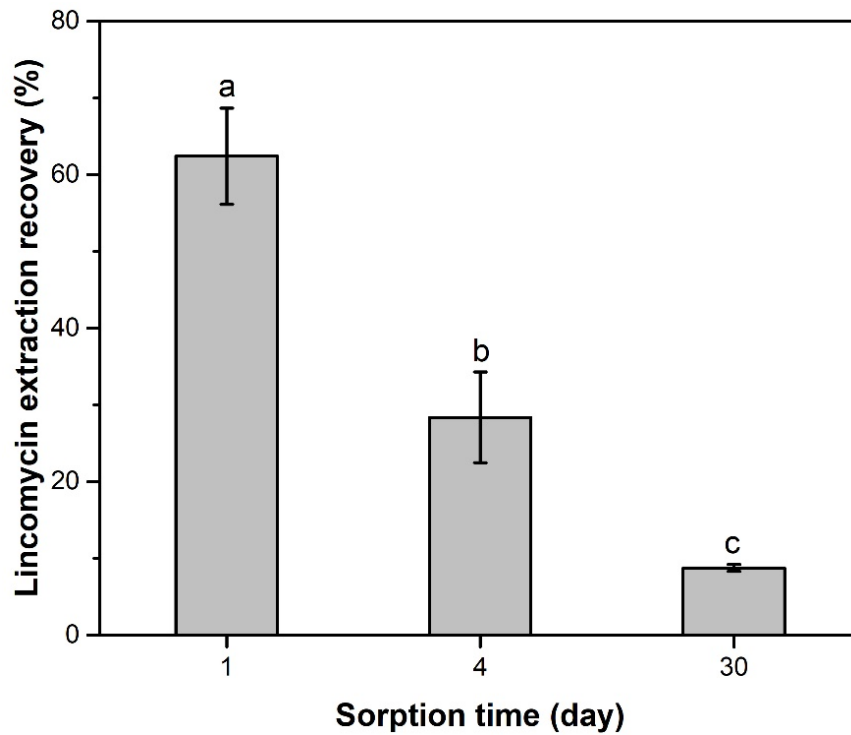


206

207 **Figure S12.** Particles size distribution of (a) bull manure biochar pyrolyzed at 300°C (BM300)

208 and (b) bull manure biochar pyrolyzed at 600°C (BM600) suspended in 0.1 M NaCl (upper

209 panel) or in 0.1 M NaOH (lower panel) after one-day exposure.



210

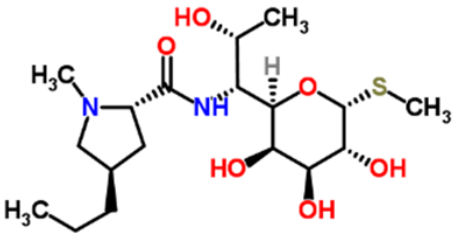
211 **Figure S13.** The effect of sorption time on lincomycin extraction recovery of DM600 biochar.

212 Means with different small letters are significantly different ($n = 2$, $p < 0.05$, one-way ANOVA

213 with post-hoc Tukey test).

214

215 **Table S1.** Physicochemical properties of lincomycin.

Chemical name	Lincomycin
Molecular structure ^a	 The chemical structure of lincomycin is shown. It consists of a 2-methyl-5-propylpyrrolidine ring connected via a carbonyl group to a 2-hydroxyethyl chain. This chain is further connected to a 2,6-dimethyl-3,4,5-trihydroxy-2-thiomethyl-β-D-glucopyranose moiety. The methyl groups on the glucose ring are highlighted in yellow, and the hydroxyl groups are highlighted in red.
Molecular formula ^b	C ₁₈ H ₃₄ N ₂ O ₆ S
Molecular weight ^b	406.537 g mol ⁻¹
Water solubility ^c	1693 mg L ⁻¹ at pH 10.0 (~100% of lincomycin exists in nonionized form)
Log octanol-water partition coefficient (log <i>K</i> _{ow}) ^b	0.20
Dissociation constant (p <i>K</i> _a) ^b	7.6

216 ^a Data from ChemSpider (<http://www.chemspider.com/>); ^b Data from TOXNET

217 (<http://www.toxnet.nlm.nih.gov/>); ^c Water solubility was estimated using Chemicalize

218 (<https://chemicalize.com/>)

219 **Table S2.** Selected properties of biochar and graphite samples.

Samples	Proximate analysis ^a			Ultimate analysis ^a				Atomic ratio		SSA ^d	V _{mic} ^e	ZP ^f
	VM ^b	Ash	FC ^c	C	O	H	N	H/C	(O+N)/C			
	%	%	%	%	%	%	%					
BM300	55.5	7.7	36.8	60.6	26.6	4.9	1.3	0.97	0.35	132	0.08	-54 ± 4
BM400	37.0	9.4	53.7	68.5	17.4	3.5	1.2	0.61	0.21	168	0.09	-50 ± 3
BM500	30.5	10.4	59.2	74.1	17.4	2.6	1.1	0.42	0.19	206	0.10	-58 ± 2
BM600	30.0	10.6	59.4	76.0	14.3	1.8	0.8	0.28	0.15	271	0.12	-57 ± 4
DM300	45.4	10.1	44.5	61.5	22.6	4.5	1.6	0.88	0.30	118	0.07	-61 ± 2
DM400	39.1	11.5	49.5	67.1	16.8	3.3	1.4	0.59	0.21	156	0.08	-58 ± 1
DM600	30.7	12.6	56.6	75.2	11.6	2.0	1.3	0.32	0.13	232	0.11	-63 ± 2
PM300	46.8	46.7	6.5	31.9	16.9	2.2	2.3	0.83	0.46	49.4	0.03	-45 ± 2
PM400	43.8	51.7	4.5	32.1	14.3	0.7	1.2	0.26	0.37	45.0	0.03	-48 ± 2
PM500	43.2	52.6	4.2	27.8	17.9	0.5	1.1	0.22	0.52	55.7	0.03	-43 ± 1
PM600	44.2	55.8	0.0	28.7	14.3	0.4	0.9	0.17	0.40	49.1	0.02	-43 ± 2
RDM500	33.0	32.0	35.0	51.2	n/a ^g	n/a	2.1	n/a	n/a	118	0.06	-52 ± 3
DDM500	42.7	14.7	42.6	59.4	n/a	n/a	2.6	n/a	n/a	116	0.06	-60 ± 3
DDM600	39.4	18.8	41.7	62.8	n/a	n/a	2.2	n/a	n/a	192	0.09	-58 ± 3
CDM500	33.0	50.1	16.9	37.8	n/a	n/a	2.0	n/a	n/a	93.2	0.05	-50 ± 3
CDMW500	25.7	58.5	15.8	74.0	n/a	n/a	0.6	n/a	n/a	135	0.06	-56 ± 3
WW500	26.9	10.9	62.1	85.9	n/a	n/a	0.4	n/a	n/a	256	0.12	-64 ± 5
Graphite	n/a	n/a	n/a	n/a	n/a	n/a	n/a	n/a	n/a	n/a	n/a	-60 ± 1

(continued on next page)

221 **Table S2. (continued)**

Samples	Total elemental analysis ^a									
	P	K	S	Ca	Mg	Na	Fe	Mn	Zn	Si
	mgkg ⁻¹	mgkg ⁻¹	mgkg ⁻¹	mgkg ⁻¹	mgkg ⁻¹	mgkg ⁻¹	mgkg ⁻¹	mgkg ⁻¹	mgkg ⁻¹	mgkg ⁻¹
BM300	3014	20017	1102	9412	3952	2712	376	137	162	213
BM400	3119	28939	859	10088	4841	3089	256	141	165	239
BM500	3115	33477	928	9432	4925	3518	267	146	167	613
BM600	2952	35820	1023	9386	5071	2937	311	165	193	146
DM300	1152	8986	1799	11094	3934	3270	208	52	90	115
DM400	1466	10345	1484	12808	4258	3569	305	53	87	112
DM600	2433	13236	1630	13997	5366	4538	398	98	114	310
PM300	26414	40013	4714	157531	8914	3868	1779	450	515	120
PM400	17957	28109	2983	265729	7164	3209	1276	397	352	n/d ^h
PM500	30555	48616	4593	204205	10436	4537	2034	566	601	n/d
PM600	23596	36775	3429	242788	8769	3457	1522	466	595	n/d
RDM500	n/a	n/a	n/a	n/a	n/a	n/a	n/a	n/a	n/a	n/a
DDM500	5649	14937	1880	18505	8498	3861	2371	162	224	n/d
DDM600	8269	20852	2863	26518	11744	5051	2356	191	200	n/d
CDM500	6011	12824	2155	38388	12534	1219	9119	542	172	198
CDMW500	n/a	n/a	n/a	n/a	n/a	n/a	n/a	n/a	n/a	n/a
WW500	270	1573	193	5427	1267	311	4208	270	93	163
Graphite	n/a	n/a	n/a	n/a	n/a	n/a	n/a	n/a	n/a	n/a

222 ^a Data adapted from Enders et al., 2012 and Rajkovich et al., 2012.; ^b VM: volatile matter; ^c FC:
223 fixed carbon; ^d SSA: specific surface area, measured by the Langmuir equation; ^e V_{mic}:
224 micropore volume, calculated using Dubinin-Astakhov equation; ^f ZP: zeta potential, sorbent
225 suspension were measured at pH 10 in 0.02 M ionic strength of background solution (6.7 mM
226 NaCl, 2.5 mM Na₂CO₃, 2.5 mM NaHCO₃, and 200 mg L⁻¹ NaN₃); ^g n/a: not available; ^hn/d: not
227 detectable.

228
229

230 **Table S3.** Fitted parameters of the intraparticle diffusion model for the long-term sorption
 231 kinetics of lincomycin by the biochars.^a

Samples	t_{ref}	k_{id}	C_{id}	R_{id}	R^2	RMSE
BM300	30	166 ± 6 a	90.6 ± 18.3 c	0.903 ± 0.008 a	0.940	72.0
BM400	180	61.7 ± 0.7 b	137 ± 4 b	0.852 ± 0.001 c	0.989	27.0
BM500	365	43.2 ± 0.2 c	115 ± 2 bc	0.876 ± 0.001 b	0.998	11.3
BM600	180	55.3 ± 0.4 b	180 ± 2 a	0.801 ± 0.001 d	0.996	14.3
DM300	90	109 ± 3 a	53.5 ± 15.1 c	0.946 ± 0.007 a	0.944	80.1
DM400	300	50.5 ± 0.8 c	145 ± 7 b	0.847 ± 0.002 b	0.975	47.4
DM600	90	88.6 ± 1.8 b	205 ± 9 a	0.789 ± 0.003 c	0.972	45.2
PM300	240	54.1 ± 0.7 a	68.6 ± 5.3 c	0.924 ± 0.001 a	0.984	34.8
PM400	365	25.3 ± 0.4 d	39.0 ± 3.8 d	0.928 ± 0.001 a	0.975	26.6
PM500	365	35.1 ± 0.3 c	162 ± 3 b	0.807 ± 0.001 b	0.993	19.0
PM600	180	49.4 ± 0.4 b	262 ± 3 a	0.719 ± 0.001 c	0.994	16.3
RDM500	180	62.1 ± 0.9 a	162 ± 6 c	0.829 ± 0.002 b	0.983	33.8
DDM500	180	62.9 ± 1 a	209 ± 6 b	0.789 ± 0.002 c	0.982	35.5
DDM600	180	44.8 ± 0.8 ce	339 ± 5 a	0.625 ± 0.002 e	0.977	28.3
CDM500	365	42.4 ± 0.3 e	124 ± 3 d	0.864 ± 0.001 a	0.994	21.9
CDMW500	300	47.5 ± 0.6 bc	162 ± 5 c	0.824 ± 0.001 b	0.987	32.3
WW500	240	48.4 ± 0.5 b	211 ± 4 b	0.768 ± 0.001 d	0.989	26.2

232 ^a t_{ref} (day) the longest time used when fitting the intraparticle diffusion model; k_{id} ($\mu\text{g g}^{-1}$
 233 $\text{day}^{-0.5}$): the intraparticle diffusion rate constant; C_{id} ($\mu\text{g g}^{-1}$): the intercept constant; and R_{id} : the
 234 intraparticle diffusion factor. Means with different small letters in the same column are
 235 significantly different ($p < 0.05$, one-way ANOVA with post-hoc Tukey test).
 236

237 **Table S4.** Fitted parameters of the Freundlich model for quasi-equilibrium sorption isotherms of lincomycin on the biochars at 1, 7,
 238 30, and 365 days. ^a

Samples	K_F				N			
	1-d	7-d	30-d	365-d	1-d	7-d	30-d	365-d
BM300	1.49 ± 0.22	30.3 ± 1.9	237 ± 8	n/a	0.727 ± 0.024 a	0.554 ± 0.012 b	0.424 ± 0.012 c	n/a
BM400	1.64 ± 0.24	5.54 ± 0.7	10.4 ± 1.7	454 ± 11	0.691 ± 0.023 a	0.626 ± 0.021 a	0.572 ± 0.027 a	0.29 ± 0.012 c
BM500	4.54 ± 0.77	7.21 ± 0.48	12.2 ± 1.1	73 ± 5.1	0.556 ± 0.027 b	0.524 ± 0.011 b	0.514 ± 0.015 b	0.483 ± 0.015 a
BM600	7.57 ± 0.61	16.4 ± 1.2	26.9 ± 1.7	282 ± 12	0.51 ± 0.013 b	0.48 ± 0.012 c	0.46 ± 0.011 c	0.325 ± 0.013 b
DM300	0.827 ± 0.186	22 ± 1.9	65.9 ± 6.6	n/a	0.69 ± 0.035 a	0.513 ± 0.015 b	0.459 ± 0.021 b	n/a
DM400	2.51 ± 0.52	4.1 ± 0.42	13.6 ± 1	146 ± 8	0.609 ± 0.031 b	0.59 ± 0.016 a	0.537 ± 0.013 a	0.48 ± 0.016
DM600	10.3 ± 1.3	38 ± 3.4	104 ± 5	n/a	0.483 ± 0.021 c	0.397 ± 0.015 c	0.369 ± 0.009 c	n/a
PM300	1.39 ± 0.24	4.68 ± 0.55	8.37 ± 0.76	215 ± 8	0.688 ± 0.027 a	0.599 ± 0.019 a	0.552 ± 0.015 a	0.407 ± 0.012 b
PM400	1.21 ± 0.23	3.22 ± 0.49	6.44 ± 0.5	20.5 ± 1.3	0.559 ± 0.029 b	0.531 ± 0.024 b	0.531 ± 0.012 a	0.524 ± 0.011 a
PM500	4.86 ± 0.54	11.2 ± 1	19.5 ± 1.3	89.7 ± 6.1	0.541 ± 0.018 bc	0.49 ± 0.014 bc	0.476 ± 0.012 b	0.402 ± 0.014 b
PM600	12.5 ± 1.5	18.9 ± 1.2	45.6 ± 3.7	312 ± 13	0.493 ± 0.02 c	0.479 ± 0.011 c	0.414 ± 0.015 c	0.348 ± 0.015 c
RDM500	6.05 ± 0.93	14.3 ± 1.6	29.4 ± 2.4	359 ± 12	0.519 ± 0.025 a	0.479 ± 0.018 bc	0.456 ± 0.014 b	0.367 ± 0.015 c
DDM500	6.76 ± 0.96	12.9 ± 0.9	38.2 ± 3.6	n/a	0.554 ± 0.023 a	0.513 ± 0.011 ab	0.413 ± 0.016 c	n/a
DDM600	15.4 ± 1.7	22.7 ± 1.7	46.4 ± 2.6	302 ± 11	0.482 ± 0.018 a	0.479 ± 0.013 bc	0.435 ± 0.01 bc	0.34 ± 0.013 c
CDM500	3.25 ± 0.73	8.3 ± 0.76	14.2 ± 1.1	77.1 ± 7	0.543 ± 0.035 a	0.523 ± 0.015 a	0.516 ± 0.013 a	0.478 ± 0.02 a
CDMW500	4.1 ± 0.79	9.38 ± 0.9	19.4 ± 2	127 ± 9	0.54 ± 0.03 a	0.511 ± 0.016 ab	0.498 ± 0.017 a	0.434 ± 0.018 ab
WW500	5.66 ± 0.95	19.8 ± 1.9	40.2 ± 3.4	187 ± 10	0.525 ± 0.027 a	0.438 ± 0.016 c	0.415 ± 0.015 c	0.403 ± 0.016 b

(continued on next page)

240 **Table S4. (continued)**

Samples	R^2				RMSE				$K_d (C_w = 1 \mu\text{g g}^{-1})$			
	1-d	7-d	30-d	365-d	1-d	7-d	30-d	365-d	1-d	7-d	30-d	365-d
BM300	0.945	0.974	0.955	n/a	14.2	36.4	68.2	n/a	1.49 ± 0.22 c	30.3 ± 1.9 a	237 ± 8 a	n/a
BM400	0.942	0.943	0.893	0.92	12.7	24.2	41	82.1	1.64 ± 0.24 c	5.54 ± 0.7 c	10.4 ± 1.7 c	454 ± 11 c
BM500	0.874	0.976	0.952	0.958	20.2	10.4	22.3	56.2	4.54 ± 0.77 b	7.21 ± 0.48 c	12.2 ± 1.1 c	73 ± 5.1 b
BM600	0.961	0.962	0.971	0.924	12.5	20.8	24.4	76.9	7.57 ± 0.61 a	16.4 ± 1.2 b	26.9 ± 1.7 b	282 ± 12 a
DM300	0.873	0.951	0.887	n/a	10.3	36	85.6	n/a	0.827 ± 0.186 c	22 ± 1.9 b	65.9 ± 6.6 b	n/a
DM400	0.854	0.957	0.969	0.957	18.1	12.8	22	59.2	2.51 ± 0.52 bc	4.1 ± 0.42 c	13.6 ± 1 c	146 ± 8
DM600	0.895	0.915	0.966	n/a	23.5	40.3	45.4	n/a	10.3 ± 1.3 a	38 ± 3.4 a	104 ± 5 a	n/a
PM300	0.922	0.946	0.959	0.957	12.7	17.5	18.5	65.2	1.39 ± 0.24 c	4.68 ± 0.55 c	8.37 ± 0.76 c	215 ± 8 b
PM400	0.858	0.889	0.968	0.978	6.21	11.5	11.4	23.9	1.21 ± 0.23 c	3.22 ± 0.49 c	6.44 ± 0.5 c	20.5 ± 1.3 d
PM500	0.939	0.952	0.966	0.929	13	17.7	22.2	67.5	4.86 ± 0.54 b	11.2 ± 1 b	19.5 ± 1.3 b	89.7 ± 6.1 c
PM600	0.907	0.971	0.931	0.914	28.2	20.4	45.7	84.9	12.5 ± 1.5 a	18.9 ± 1.2 a	45.6 ± 3.7 a	312 ± 13 a
RDM500	0.876	0.919	0.946	0.912	20	27.4	35.3	86.3	6.05 ± 0.93 bc	14.3 ± 1.6 b	29.4 ± 2.4 c	359 ± 12 a
DDM500	0.905	0.973	0.922	n/a	24.3	17.2	42.7	n/a	6.76 ± 0.96 b	12.9 ± 0.9 bc	38.2 ± 3.6 b	n/a
DDM600	0.917	0.957	0.97	0.915	29.9	28.8	33.3	92.6	15.4 ± 1.7 a	22.7 ± 1.7 a	46.4 ± 2.6 a	302 ± 11 b
CDM500	0.791	0.954	0.962	0.915	17.9	16.4	22.6	81.5	3.25 ± 0.73 c	8.3 ± 0.76 c	14.2 ± 1.1 d	77.1 ± 7 e
CDMW500	0.834	0.947	0.935	0.93	19	18.2	34.6	79.3	4.1 ± 0.79 bc	9.38 ± 0.9 c	19.4 ± 2 d	127 ± 9 d
WW500	0.86	0.926	0.927	0.915	21	26.6	43.1	79.9	5.66 ± 0.95 bc	19.8 ± 1.9 a	40.2 ± 3.4 ab	187 ± 10 c

241 ^a $K_F (\mu\text{g}^{1-N} \text{g}^{-1} \text{L}^N)$: Freundlich sorption coefficient; N (dimensionless): Freundlich nonlinearity factor; $K_d (\text{L g}^{-1})$: sorption distribution
242 coefficient; $C_w (\mu\text{g L}^{-1})$ is the dissolved lincomycin concentration in the solution phase; and n/a: fitted parameters were not available
243 because the concentrations of lincomycin in solution were below detection limit. Means with different small letters in the same
244 column are significantly different ($p < 0.05$, one-way ANOVA with post-hoc Tukey test).

245
246

247 **Table S5.** Fitted parameters of the intraparticle diffusion model for the sorption kinetics of
 248 lincomycin by woodchip waste biochar. ^a

Samples	t_{ref}	k_{id}	C_{id}	R_{id}	R^2	RMSE
WW500+DI	60	55.2 ± 0.4 a	178 ± 1.8 a	0.705 ± 0.001 b	0.997	7.80
WW500+DOC(BM300)	60	13.3 ± 1.2 d	80.3 ± 5.4 b	0.535 ± 0.0014 e	0.678	23.3
WW500+DOC(DM300)	60	29.1 ± 0.9 b	70.5 ± 3.9 b	0.767 ± 0.006 a	0.951	16.8
WW500+DOC(PM300)	60	15.0 ± 1.2 d	71.1 ± 5.2 b	0.598 ± 0.015 d	0.743	22.5
WW500+DOC(DDM500)	60	23.1 ± 0.9 c	85.6 ± 3.7 b	0.648 ± 0.007 c	0.931	16.0

249 ^a t_{ref} (day) the longest time used when fitting the intraparticle diffusion model; k_{id} ($\mu\text{g g}^{-1}$
 250 $\text{day}^{-0.5}$): the intraparticle diffusion rate constant; C_{id} ($\mu\text{g g}^{-1}$): the intercept constant; and R_{id} : the
 251 intraparticle diffusion factor. Means with different small letters in the same column are
 252 significant different ($p < 0.05$, one-way ANOVA with post-hoc Tukey test).
 253

254 **Table S6.** Fitted parameters of the intraparticle diffusion model for the sorption kinetics of
 255 lincomycin by raw-, DI-water-washed, and 0.01M-NaOH-washed biochars. ^a

Samples	t_{ref}	k_{id}	C_{id}	R_{id}	R^2	RMSE
BM300-Raw	30	160 ± 4 b	87.9 ± 13.8 c	0.904 ± 0.003 a	0.968	47.1
BM300-DI	15	166 ± 1 b	285 ± 1 b	0.694 ± 0.001 b	1.000	3.56
BM300-NaOH	7	176 ± 5 a	527 ± 10 a	0.460 ± 0.003 c	0.985	18.7
DM300-Raw	60	113 ± 2 c	49.8 ± 8.0 c	0.945 ± 0.004 a	0.984	34.6
DM300-DI	30	148 ± 2 b	99.1 ± 7.6 b	0.894 ± 0.005 b	0.990	24.1
DM300-NaOH	10	172 ± 1 a	381 ± 1 a	0.587 ± 0.001 c	1.000	3.26
PM300-Raw	60	51.3 ± 1.5 b	83.1 ± 2.1 b	0.831 ± 0.002 a	0.995	8.93
PM300-DI	60	68.1 ± 1.5 a	131 ± 6 a	0.811 ± 0.004 b	0.976	25.4
DDM500-Raw	60	74.1 ± 0.8 b	164 ± 3 b	0.781 ± 0.002 b	0.994	13.8
DDM500-DI	60	98.5 ± 0.5 a	191 ± 2 a	0.800 ± 0.001 a	0.999	9.05
BM600-Raw	60	53.8 ± 0.6 b	174 ± 3 b	0.710 ± 0.002 a	0.993	11.0
BM600-DI	60	52.2 ± 0.9 b	175 ± 4 b	0.705 ± 0.003 a	0.983	16.3
BM600-NaOH	60	55.9 ± 0.5 a	203 ± 2 a	0.685 ± 0.002 b	0.996	8.48

256 ^a t_{ref} (day) the longest time used when fitting the intraparticle diffusion model; k_{id} ($\mu\text{g g}^{-1}$
 257 $\text{day}^{-0.5}$): the intraparticle diffusion rate constant; C_{id} ($\mu\text{g g}^{-1}$): the intercept constant; and R_{id} : the
 258 intraparticle diffusion factor. Means with different small letters in the same column are
 259 significantly different ($p < 0.05$, one-way ANOVA with post-hoc Tukey test).
 260

261 **References for Supplementary Material**

- 262 Chuang, Y.H., Zhang, Y., Zhang, W., Boyd, S.A., Li, H., 2015. Comparison of accelerated
263 solvent extraction and quick, easy, cheap, effective, rugged and safe method for extraction
264 and determination of pharmaceuticals in vegetables. *J. Chromatogr. A* 1404, 1-9.
- 265 Enders, A., Hanley, K., Whitman, T., Joseph, S., Lehmann, J., 2012. Characterization of biochars
266 to evaluate recalcitrance and agronomic performance. *Bioresour. Technol.* 114, 644-653.
- 267 Liu, C.H., Chu, W.Y., Li, H., Boyd, S.A., Teppen, B.J., Mao, J.D., Lehmann, J., Zhang, W.,
268 2019. Quantification and characterization of dissolved organic carbon from biochars.
269 *Geoderma* 335, 161-169.
- 270 Rajkovich, S., Enders, A., Hanley, K., Hyland, C., Zimmerman, A.R., Lehmann, J., 2011. Corn
271 growth and nitrogen nutrition after additions of biochars with varying properties to a
272 temperate soil. *Biol. Fertil. Soils* 48(3), 271-284.
- 273 Sigmund, G., Huffer, T., Hofmann, T., Kah, M., 2017. Biochar total surface area and total pore
274 volume determined by N₂ and CO₂ physisorption are strongly influenced by degassing
275 temperature. *Sci. Total Environ.* 580, 770-775.

276